The impact of a downslope water-transport parameterization in a global ocean general circulation model

Stephanie Legutke and Ernst Maier-Reimer

Max-Planck-Institut für Meteorologie
Bundesstraße 55, D-20146 Hamburg

ISSN 0937-1060

Abstract

The impact of a downslope water-transport parameterization on the circulation and water mass characteristics of a global depth-level ocean general circulation model (OGCM) is investigated. The spreading of dense water from the formation regions into the deep ocean is known to be poorly represented in depth-level models with no bottom boundary layer resolved or attached. The new scheme is simple and intends to parameterize the effects of various oceanographic processes (rather than the processes themselves) that help dense water to descend topographic slopes by which the formation regions are separated from the world ocean. The new scheme significantly improves the large scale properties of the North Atlantic Deep Water (NADW). Changes in the North Atlantic circulation, however, are rather small. In the Southern Ocean, the exchange between the dense water formation regions on the continental shelves and the deep ocean is strengthened at the expense of deep water mass formation by open ocean convection. In all three ocean basins, the density of the deep and bottom water is higher with the new parameterization, which brings the simulations closer to observations in the Atlantic and Indian Oceans. In the Pacific Ocean, however, where the density has already been well reproduced without the downslope transport, it gets slightly too high. The results are in agreement with those from other model studies.

1 Introduction

The densest water masses in the world ocean are formed in semi-enclosed basins separated from the abyssal seas by steep continental slopes or submarine ridges. In order to contribute to the ventilation of the deep ocean, the dense water has to descend the slopes or to flow over the ridges.
In the southern hemisphere, the most important dense water formation regions are the Antarctic continental shelves. Densification of surface water there occurs through cooling either by the atmosphere or by melting of ice shelves, and through increase of salinity by release of brine during the formation of sea ice. Downslope flow of dense shelf water has been observed in the Weddell and Ross Seas, and traces of such flow have been found all along the Indian Ocean sector of the Antarctic shelves (Baines and Condie 1998). When the water flows down the slope, it mixes with the overlying warmer and saltier Circumpolar Deep Water (CDW) (Foster and Carmack 1976). The mixing product, the Antarctic Bottom Water (AABW), ventilates the abyss of the world ocean (Luyten et al. 1993, Rintoul 1998).
The source water of CDW, the NADW, is also a product of mixing processes which involve dense bottom water flowing over steep topographic slopes. The associated dense waters originate north of the Greenland-Scotland ridges. Most of it leaves the Greenland and Norwegian Seas through the Denmark Strait and the Faeroe Bank Channel, but some water flows also over the sills between Iceland and the Faeroe Islands. This overflow water mixes with overlying water masses, in particular with Labrador Sea water (Dickson and Brown 1994), but derivatives of AABW and of saline water of Mediterranean origin contribute as well (Rhein and Hinrichsen 1993).
The latter again contain a dense slope water mass, the Mediterranean outflow, which descends the continental break west of the Strait of Gibraltar. It mixes with the overlying North Atlantic Central Water whereby it looses much of its density (Price et a. 1993) and also helps to precondition the Atlantic inflow to the Arctic Ocean for deep water formation (Reid 1979).
Although it has been argued that cold brine-enriched shelf water must transport salt into the deep Arctic Ocean to explain the high salinity there (Aagaard et al. 1985), formation of dense deep or bottom water at high northern latitudes is much less evident. Schauer et al. (1997) see the reason in the more efficient dilution of Arctic shelf water by continental runoff. Observed traces of dense slope plumes in the European Arctic indicate penetration depths of 1000 m to 2300 m only. For the Canadian Basin, Rudels et al. (1994) explained the characteristics of deep and intermediate water by plumes descending from the shelf while entraining water from the slope boundary current.

The layer thickness of observed downslope flow is O(10 m) to O(100 m) and the flow is often intermittent in time (Dickson and Brown 1994). Thus, direct observations of the descent of dense water are rare, and most of our knowledge about the dynamics of downslope flow has been deduced from high-resolution regional or idealized numerical ocean models, or from laboratory experiments. Price and O'Neil Baringer (1994) examined the outflow from the Mediterranean Sea, the Filchner Ice Shelf, and the Greenland-Norwegian Seas. They note in particular that the density ordering of the water masses at the

time when they are formed is the reverse of the density ordering of the final products when these have settled into the deep ocean. Price and O'Neil Baringer (1994) conclude that entrainment of ambient water into the bottom layer varies considerably between the different regions. It is also known from observations that entrainment is variable in intensity even along the path of one water mass, e.g. the Mediterranean outflow (Price et al. 1993, Dickson and Brown 1994).
In their simulation of bottom flow with stream-tube models, Price and O'Neil Baringer (1994) considered entrainment in the dynamics of the stream by making it dependent on the density difference between the bottom water and the ambient water, the thickness of the bottom layer, and its velocity. Using the appropriate parameters for each of the outflow regimes, they were able to simulate the main characteristics of the flow. A crucial parameter for the entrainment in their models is the local bottom slope, which is scale dependent. Another aspect of the model of Price and O'Neil Baringer (1994), which has a significant impact on the results, is the parameterization of the broadening of the stream-tube. It includes the bottom drag coefficient, which is assumed to depend on the surface roughness. A further important aspect is the thermobaric effect (Killworth 1977). It can accelerate the descent, and the dense water can reach deeper before it settles at its level of neutral density. The larger velocity, on the other hand, can cause stronger entrainment and thus neutralize the thermobaric acceleration (Jungclaus et al. 1995).

Baines and Condie (1998) summarize the results of recent modeling activities with high-resolution 3D-models of shelf regions. These models show that the frontal currents which evolve by the geostrophic adjustment process after convective formation of dense water can be extremely unstable. Offshore transport of dense water is controlled by baroclinic eddies which accompany the adjustment process. In addition, downslope Ekman drainage from the dense bottom layer may cause eddies to form by vortex stretching of the water column above the dense layer. The thinner the latter the more stable the flow. The relative importance of downslope transport by eddies or by Ekman flow depends on the ratio of the Ekman layer depth and the depth of the dense layer. Baines and Condie (1998) characterized flow regimes by a non-dimensional parameter involving the bottom slope, the Coriolis parameter, the dense water production rate per unit length of the slope, the density difference, and the turbulent vertical eddy viscosity. Flow characteristics can thus change in the downstream direction by detrainment and entrainment, local changes in bottom topography and bottom roughness, as well as by changes of the strength of the dense water source. The bottom friction coefficient has also been found to be the most important parameter in the model of Jungclaus et al. (1995). Together with small scale features of the topography it has significant influence on the flow path.
The downslope transport increases when the models include small-scale canyons cutting through the shelf slope. These canyons may accelerate the descent of the dense water by geostrophically channelling the fluid downslope (Jungclaus and Mellor 1999). On the other hand, as with the thermobaric effect, the fluid may find its level of neutral density at a higher level due to the increased velocity and associated larger entrainment rates.

Another process which can influence downslope transport of dense water is the occurrence of turbidity currents due to suspended sedimentary materials which increase the density of the bottom water (Fohrmann et al. 1998).

OGCMs that have their levels of computation at horizontal surfaces, depth-coordinate or z-level models as they are called, are widely used in coupled climate models. When dense water is formed in these models on the shelves, it tends to stay there instead of flowing downslope, since global depth-coordinate models normally do not resolve the processes which control downslope flow (e.g. baroclinic eddies, Ekman layer dynamics). Downslope transport of dense water in z-level models is described as a stepwise procedure of alternating horizontal and vertical transports. The transport can be diffusive or advective in both directions. In the vertical direction, there is an additional downward transport of tracers by convective adjustment, which is used to remove vertical instabilities by temporarily increased vertical diffusion. Dense water that descends a slope thus undergoes strong dilution with lighter water found offslope. The deep and bottom water in depth-coordinate models is then often too light when it has reached the bottom (Campin and Goose 1999, Danabasoglu and McWilliams 1995). This has severe consequences for the ventilation of the deep ocean and thus the applicability of such models in climate change studies. A remedy to this problems, which has frequently been used, is to artificially increase the density of the water in the formation regions above observed values, so that even with a too strong mixing with lighter water, the descending water has about the right density when it arrives at the bottom (Toggweiler and Samuels 1995, England 1993). This approach, however, is not appropriate in climate change studies, where the prediction of surface conditions in dense-water formation regions is an essential prerequisite for a prediction of ventilation changes in the deep ocean and thus of the long-term response of the climate system.

The sensitivity of this response to the formulation of the downslope transport of tracers can be large, as has been shown by Lohmann (1998) with an idealized model of the Atlantic Ocean coupled to an energy-balance model of the atmosphere. Lohmann (1998) added a 'slope convection' term to the tracer transport equations of the grid cells nearest to the bottom, as was proposed by Beckmann and Döscher (1997). He showed that the sensitivity of the thermohaline circulation of the coupled system to a perturbation of the surface salinity south of the Greenland-Scotland ridge system was reduced with the 'slope convection' included. Lohmann (1998) concluded that depth-coordinate ocean models might be too sensitive to changes of the surface forcing in the North Atlantic.

Improvement of the downslope transport in depth-coordinate ocean models is therefore needed in order to increase their reliability in climate studies. Most of the model-development activities in this respect has been undertaken with idealized ocean basins.
Killworth and Edwards (1999) implemented a bottom boundary layer with spatially and temporarily changing height into a depth-coordinate ocean model. Entrainment and detrainment was included, based on a formulation for the equilibrium depth of turbulent boundary layers and on the boundary-layer height calculated in the model from divergence and convergence in the bottom layer. Since the bottom boundary

layer is based on the full standard Boussinesq Navier-Stokes equations with the pressure gradients formulated within the bottom layer, the finite-difference formulation invokes pressure-gradient errors of the kind known from terrain-following σ-coordinate models. In order to minimize these errors, Killworth and Edwards (1999) removed depth-dependencies from the equation of state. For the test case of a periodic channel with southward increasing water depth in the northern half of the channel, the model produced significant downslope flow, while in the same model with no bbl, the dense water was trapped on the shallow part of the basin.

The complex formulation of Killworth and Edwards (1999) is not easily included into an existing model code. Secondly, problems can arise with a prognostic height of the bottom layer when the height becomes larger than half of the bottom cell. In global OGCMs this is most likely to occur in the shallower layers, where the vertical resolution is commonly specified to be higher in order to account for the larger vertical variations in density. With the present computing facilities, even OGCMs used in climate studies have a layer thickness of O(10 m) in the upper ocean. Thus, problems are likely to occur in regions where sill depths are shallow. In the model used in this study, the sill depth of the Strait of Gibraltar is at about 200 m. Above this level all layers are thinner than 75 m. The situation is even more critical in the Bering Strait (sill depth about 75 m), there however, dense bottom flow does not seem to be crucial for the thermohaline circulation and global deep water properties.

Gnanadesikan (1997, unpublished manuscript) also tested a formulation of a bbl which used the full equations to calculate direct flow between the bottom layer cells. The formulation of the pressure gradients within the bottom layer thus also gave rise to spurious pressure gradients in the discretized version of the equations. By disallowing the height of the bottom cell to vary in time or space though, he avoided potential problems of the bottom layer becoming too thick. With a pre-specified layer thickness, turbulence is modeled with a turbulence coefficient rather than with de/entrainment. This model also satisfactorily treated the downslope flow in idealized test cases with specified regions of dense water formations. Sensitivity studies of the influence of the specified bbl height, however, showed a rather high impact of this parameter on the model results.

Beckmann and Döscher (1997) avoided the problems with the horizontal pressure-gradient errors in terrain-following bbl-coordinates by only calculating tracer tendencies in the bbl. The velocities and tracer distribution entering these equations are calculated in depth-coordinates. This requires the bottom layer to fill the whole grid cell above the bottom. The coupling to the interior cells is done by using a weighted average of the tracer tendencies calculated in depth-coordinates and those calculated in the bbl. With this model, Beckmann and Döscher (1997) showed that a coarse-resolution version with bbl formulation simulated dense plumes on a sloping bottom with shape and path similar to those in a higher-resolution version with no bbl and to those in a σ-coordinate model version. In the coarse-resolution version of the model with no bbl, the dense water showed a stronger tendency to follow isobaths and was more efficiently trapped in the shallow region of the model basin.

In global OGCM used in climate studies, the velocities near the bottom are rather weak due to their coarse resolution. Therefore, Beckmann and Döscher (1997) also run a test case where only the additional diffusion in bbl-coordinates was activated and no modification of tracer tendencies by advection within the bbl was applied to the interior tracer equations. The diffusion coefficient was different from zero only when the condition for 'slope convection' was fulfilled, i.e. when the upper bottom cell contained the denser water. Even with this purely diffusive bbl formulation, a more realistic spreading of plumes above bottom slopes was obtained.

The parameterizations described above were implemented and tested in idealized basins only. In global OGCMs with realistic topography additional problems might occur as already noted. In addition, these models have a horizontal resolution of no more than O(100km), while in the test cases described above, grid sizes of O(10 km) were used.

Campin and Goose (1999) describe the first implementation of a bbl parameterization into a global OGCM with realistic topography. As in Beckmann and Döscher (1997) they consider the entire bottom cell to constitute the bbl and modify only tracer tendencies. Downslope velocity is not taken from the basic model, however, but is calculated from a balance between the downslope pressure gradient (on horizontal surfaces) and a linear bottom drag. Since only downslope velocities are added to the tendency equations, a compensating flow is specified to occur immediately above the lower bottom cell involved in the mixing. The downslope transport is proportional to an additional parameter which should ideally depend on the local bottom slope and the surface roughness. By obvious reasons it is taken to be constant by Campin and Goose (1999).

Here we describe the impact of a downslope tracer transport scheme in another global OGCM with realistic topography. The parameterization is similar to the 'slope convection' case described by Beckmann and Döscher (1997). It is similar to that of Campin and Goose (1999), in that the whole bottom cell belongs to the bbl. It differs from that formulation in that the transport is considered to be a directional turbulent exchange. The implementation is similar to the vertical convective adjustment used in OGCMs, and thus no additional tuning parameter is introduced. The rationale behind the search for a parameterization as simple as possible, which however helps to improve the deep water properties in global OGCMs, is that most of the above mentioned processes which influence downslope transport (small scale topography and bottom roughness, eddies, sediments, local density gradients near the bottom) are not resolved in OGCMs. We thus do not aim at parameterizing any of these processes, but rather their overall effect on the large scale water mass properties. I.e., we hope to improve the deep ocean stratification and circulation by reducing the dilution of deep dense water on its downslope descent and by increasing the strength of the exchange between the formation regions and the deep ocean. The model has a somewhat finer resolution than that of Campin and Goose (1999). It differs in many other aspects as well, the main difference being the incorporation of a fully prognostic sea ice model and the forcing with high-frequency instead of annual-mean data. This allows to explicitly simulate the formation of

dense water at the surface instead of artificially increasing the surface density. The model, the bbl parametrization, and the experiment setup is described in the next section. The climatological state of the ocean simulated with and without the bbl parameterization are compared in Section 3. Conclusions and a summary are given in Section 4.

2 Description of the ocean model and the experiment

The model used in the present study is a global version of the Hamburg Ocean Primitive Equation GCM (HOPE-G). Variants of the model have been used in studies of the global ocean general circulation (Drijfhout et al. 1997, Stössel and Kim 1998), in regional studies (Legutke 1991, Marsland and Wolff 2000), and in studies of the coupled atmosphere-ocean system (Luksch and von Storch 1991, Frey et al. 1997). Simulations with the present model version are presented in Legutke et al. (1997) and Legutke and Maier-Reimer (1999). The numerical model formulation is described in detail in Wolff et al. (1997). The model equations are discretized on a Gaussian grid (T42, ca. 2.8^o) with 20 horizontal surfaces at 10, 30, 51, 75, 100, 125, 150, 175, 206, 250, 313, 425, 600, 800, 1050, 1450, 2100, 3000, 4000, 5250 m. The concentration of the model levels in the upper ocean and an additional refinement of the horizontal grid in the meridional direction on both sides of the equator serve to improve the representation of the highly variable thermocline, in particular in the tropical oceans. A good resolution of the topography is guaranteed despite the large distances between levels at large depths, since the model discretization allows for partial vertical grid cells at the bottom (see e.g. Figure 3). Thereby, the resolution of the bottom topography is limited by the horizontal resolution of the grid only, and not by the number of computational levels. The baroclinic pressure is always computed at a constant depth for each layer, and thus does not induce spurious bottom-pressure terms. It has been shown that this formulation gives a smoother flow field above topographic features than models with a comparable number of layers and full vertical cells (Adcroft et al. 1997).

The model domain includes the Mediterranean Sea, as well as the Hudson and Baffin Bays, and the Baltic Sea. The Arctic Ocean is connected to the Pacific by the Bering Strait, and to the Atlantic by the Denmark Strait and the Iceland-Scotland passages. The exchange of water, heat, and salt between the peripheral seas and the world ocean is dynamically computed by solving the full set of model equations. Small scale features, however, as e.g. eddies are not resolved there or in other parts of the model domain. Their effect on the large scale circulation is parameterized by assuming vertical and horizontal 'eddy' diffusion and viscosity coefficients which depend on the density stratification and the velocity shear. At solid boundaries, no-flux conditions are specified for tracers, and no-slip conditions for momentum. Near the bottom, a linear Raleigh friction is included, in addition to increased vertical eddy viscosities. At the surface, a turbulent deepening of the mixed-layer is parameterized by increasing the vertical eddy diffusivity and viscosity coefficients when the density stratification becomes weak. Mixed-layer deepening by buoyancy fluxes through the surface is accounted for by vertical mixing of the unstable part of the

water column, the so-called convective adjustment, a common parameterization of convection in hydrostatic ocean models. Convection occurs most frequently in high latitudes where it is triggered by surface cooling or increase of surface salinity due to sea ice formation (Figure 1 and Figure 5).
As usual in z-level models, the transport of tracers from one grid cell to the next in the default version of the model is calculated by alternating purely horizontal or vertical exchanges between neighboring grid cells as described above. Thereby, dense bottom water descending a slope is diluted with light ambient water to a larger extent than seems appropriate. As a consequence, the dense water becomes too light when it flows over the ridges and downslope into the deep ocean (Figure 2c and Figure 9).
This problem is common to many other efforts of simulating the climate of the world ocean (e.g. Campin and Goose 1999). It can be disguised by applying so-called 'salinity enhancement' near the continental margin of Antarctica. In such attempts the salinity at the surface near the coast is restored to high values in order to mimic the impact of sea ice formation on the surface salinity and to improve the deep water mass properties. This method has been criticized since the salt flux involved might correspond to sea ice formation rates much larger than those deduced from observations (Toggweiler and Samuels 1995). The model described here contains a state-of-the-art sea ice model. It accounts for sea ice dynamics by solving a two-dimensional momentum equation for the sea ice velocity which includes interfacial stress at the upper and lower surface of the ice flows and an internal ice resistance to shear and compression based on a viscous-plastic rheology as described by Hibler (1979). Thermodynamically, the sea ice cover is treated as an insulating two-dimensional slab with linear vertical temperature profile and a salinity corresponding to 5 psu. The insulating property of the ice cover is enhanced by a snow cover which also changes the surface albedo. Surface melting occurs when the skin temperature of the snow rises above melting point. The skin temperature is calculated with a surface heat budget similar to that described by Parkinson and Washington (1979), using near-surface conditions taken from a 15-year integration of the ECHAM4 atmosphere general circulation model (Roeckner et al. 1996). Daily fields are used to account for the non-linear dependence of surface fluxes (and thus deep water formation rates) on the near-surface conditions in the atmosphere. The forcing is cyclically repeated every 15 years. The sea ice cover is fractional thus accounting for the large differences of heat fluxes over sea ice and water. Continuity equations are solved for ice thickness, concentration, and snow depth.
A mismatch between the surface fluxes required by coarse standalone ocean and atmosphere models to simulate a realistic climate requires additional fluxes of heat and freshwater. These are obtained by restoring the surface salinity and temperature in the ocean to observed values on a time scale of one month. The additional freshwater fluxes, however, are not applied in ice regions (defined by monthly observed ice extent) in this model in order to have the salinity changes in the upper ocean exclusively prognosticated by the simulated ice formation and the freshwater fluxes of the atmosphere model. The SSS relaxation in the Southern Ocean mainly serves to keep the upper ocean stratified equatorwards of the ice edges, i.e. the freshwater fluxes are downward, in contrast to the 'salinity enhancement' which corresponds to upward freshwater fluxes. The model has a free surface, so that freshwater fluxes through

the surface can be applied directly with exact conservation of salt. Restoring of salinity outside ice regions is achieved by the application of a freshwater flux that brings the surface salinity to the required value.
The climatology obtained with the same forcing as the one used here is described in Legutke and Maier-Reimer (1999). It is shown that the model simulates a reasonably realistic annual state and seasonal cycle within the limits given by the resolution of the model grid. The simulated climatology suffers, however, from the above-described deficiencies of the representation of the downslope descent of dense water. A simple bbl parameterization has now been implemented in the model and a new integration with the bbl included is performed, which is the subject of this paper. The results will be compared with a corresponding simulation without bbl, which will be called 'control' experiment.

The approach is similar to the one adopted by Campin and Goose (1999). The ocean model, however, is different from that of Campin and Goose (1999) in many respects (horizontal and vertical grid resolution, partial bottom grid cells, parameterization of subgrid-scale mixing, explicit formation of dense water instead of restoring temperature or salinity to extreme values in the formation seasons, inclusion of a sea ice model). It will thus be possible to comment on the dependency of the impact of a bbl on the model formulation.

The bbl parameterization of HOPE-G differs from that of Campin and Goose (1999) in that it is formulated as a downslope convection similar to the 'slope convection' proposed by Beckmann and Döscher (1997). The water of two horizontally adjacent bottom cells is mixed if the cells belong to different layers of the grid and if the higher cell contains the denser water. The model uses the UNESCO equation of state. It therefore accounts for the nonlinearity of the equation of state and the thermobaricity of sea water. The comparison of density in two cells which are potentially mixed is done relative to the depth of the upper horizontal surface of the lower cell. The diffusion coefficient depends on the local geometry. It is proportional to 1/l where l is the number of neighboring bottom cells that belong to a lower layer, i.e. the number of potential downslope pathways of the water in the cell in consideration. Besides this factor, the diffusion coefficient is set locally to the maximum allowed values, i.e. when there is just one way down, half of the volume of the smaller cell (in most cases the upper cell) is exchanged. If there are two lower neighboring cells, half of the volume of the upper cell is mixed with these cells, provided, the lower cells have the lower density. This makes the downslope mixing similar to the formulation of the vertical adjustment process in the model and no new parameter need to be introduced. In both cases, the success of the parameterization is evaluated by its overall effect on the model climate, rather than by the accuracy of the representation of the simulated processes. Neglecting the advective aspects of the slope flow and representing it as a directional turbulent process within the bottom cells, it is assumed that the slope flow is of small scale and that the return flow is within the same grid cells. Thereby, ad hoc assumptions on where the return flow takes place are avoided. Campin and Goose (1999), using an advective formulation, specify the return flow to occur in the water column above the deeper cell being involved.

If this column is density stratified, this involves a flow against the potential energy barrier.
It is not checked whether the water parcel can reach its level of neutral density already on a higher level than the next bottom cell. Thus, only water is mixed downward that would reach the next bottom plateau in the model grid in the absence of entrainment. However, the difference between the total number of layers in neighboring columns is larger than 1 in only 3% of all cases. Thus, the number of vertical steps the water can overcome in one swap does not make a big difference for the model results.
If the density in the bottom cell is not larger than in the downslope cells, the water can 'detrain' from the bottom layer by horizontal diffusion or advection.

Both simulations described here have been run for 709 years at which time the model has almost achieved a steady-state. If not specified otherwise, the model results represent 15-year means of the last forcing cycle. Both experiments have been started from a state of rest with the temperature and salinity stratification specified by the Levitus climatology (Levitus et al. 1994).

3 Results

Slope convection is associated with a change of potential energy in the water columns involved. The global difference pattern of the potential energy change between the control experiment and the experiment including the bbl parameterization (not shown) reveals that significant changes of downslope and vertical convection are found only in the downstream direction of the Denmark Strait, south of Iceland, in the Strait of Gibraltar, and on the continental margins of the Southern Ocean. These are the regions where significant downslope flow has been observed (Price and O'Neil Baringer 1994). They also roughly correspond to the regions where downslope transports are largest in the model of Campin and Goose (1999).

The differences of the potential energy released by vertical convection in the two experiments are shown in Figure 1a for the North Atlantic. Southeast of Greenland, vertical convective activity is clearly increased near the coast. This is a consequence of the downslope convection process, which transports dense bottom water to deeper levels, as indicated by the dipole pattern in Figure 1b, which shows the potential energy change by downslope convection in the bbl experiment. The change of potential energy resulting from a downslope convection event is negative in the upper cell and positive in the lower cell (besides effects of the nonlinearity of the equation of state and thermobaricity). Downslope convection reduces the vertical stability in the shallower column (e.g. on the shelf). When the water is cooled at the surface, it is more readily mixed with the underlying relatively warmer water. The total exchange between Greenland and Scotland is 4.4/-5.7 Sv in/outflow in the bbl experiment, and 4.5/-5.9 Sv in/outflow in the control experiment. Of the latter, 3.9 and -4.2 Sv go through gaps between the Iceland and Scotland Ridge (1 Sv=1 $10^6 m^3 s^{-1}$). The net southward flow is due to a northward flow of 1.21 (1.3 Sv) through the Bering Strait and precipitation and continental runoff into the Arctic Ocean in the bbl (control) experiment. There is thus little change of volume transport in this region by the bbl parameteriza-

tion, in agreement with other model sensitivity studies (Lohmann 1998, Campin and Goose 1999). The total values of both experiments lie within the range obtained by direct or indirect observations. However, the real outflow seems to be partitioned into equal parts east and west of Iceland (Dickson and Brown 1994).

Some vertical convective activity also occurs in the Strait of Gibraltar. However, the absolute values in both experiments, as well as their differences, are small compared to those in other sites (Figure 1a).

There is some downslope 'flow' in the Kara Sea, though with small impact for the potential energy (Figure 1c). In the depth range 150 m to 400 m in the Arctic Ocean, however, where this downslope convection occurs, the warm temperature bias (ca. 0.5^{o}C) of the control experiment is reduced by about 40% in the bbl experiment (not shown). At other depths, the temperature profile remained unchanged, as does the salinity profile at all depths. In the deep Norwegian Sea, the difference pattern of the total potential energy change has negative values (Figure 1c) because of increased stability in the North Atlantic Water (NAW) and reduced vertical convective adjustment in the bbl experiment.

In the control experiment, the regions of most intense vertical mixing activity are the Labrador Sea south of Greenland, the Faeroer Shetland Channel, and the Norwegian Sea (Legutke and Maier-Reimer 1999). The deep water formation rates by vertical mixing there are essentially unchanged by the bbl parameterization (Figure 1a).

The overall effect of the new parameterization on the salinity and temperature stratification in the central North Atlantic is demonstrated in Figure 2. The positive temperature error in 1000 m depth is decreased from about 2^{o}C to 0.75^{o}C. The salinity error is also reduced by about 50%. These improvements are not only due to the formation of a fresher deep water mass in the Northern North Atlantic by a larger addition of fresh slope water. A large effect also comes from an improvement of the downslope flow out of the Mediterranean. Without the bbl parameterization, the largest salinity is found at about 800 m depth. With the bbl included, the outflow reaches its level of neutral density near the strait at 1050 m, where it is also found in the observations. In addition, the exchange through the strait is reduced from 0.86/-0.83 Sv to 0.65/-0.63 Sv. While the volume exchange of the experiment without bbl seems to agree better with observations (Bryden and Kinder 1991), the large scale salinity distribution is better reproduced with the bbl parameterization included (Figure 2 and Figure 3). Though both temperature and salinity are improved near 1000 m, the density error has become slightly larger there (Figure 2c). Error compensation does not work as good as with the control run results.

Figure 3 shows the zonal mean salinity differences of the two simulations in the Atlantic Ocean. It is in many aspects similar to the results of Campin and Goose (1999). Both models show a decrease of salinity (by ca. 0.2 psu) at intermediate depths in the North Atlantic. In HOPE-G, the minimum at 30 N is due to the modified influence of the Mediterranean water, which is also responsible for the slight increase of salinity at 1300 m depth. The second minimum at 45 N is due to the larger contribution of fresh Greenland Sea water to the NADW. A significant difference to the results of Campin and Goose (1999) exists below 2000 m between 30 N and 60 N. The freshening in the deep North Atlantic in HOPE-G stems from

an increase of AABW inflow from the south which pushes the saltier NADW upwards. The ventilation rate of the deep Atlantic by AABW has increased from about 3 Sv to 4 Sv (not shown) and agrees well with those given by Luyten et al. (1993). In the model of Campin and Goose (1999) the pattern is similar but with positive sign possibly due to an increase of salinity of the overflow water. In HOPE-G, the overflow water is slightly fresher (Figure 3).

Both models show a general freshening of the deep Atlantic due to a more efficient ventilation with AABW, and an increase of salinity near the Antarctic continental slope. At this point, however, a model intercomparison is not straightforward. Campin and Goose (1999) use salinity enhancement near the coast which keeps the shelf salinities at high values independent from other flow characteristics. Increased salinities on the slope in HOPE-G stem from less dilution of brine-enriched shelf water during the downslope descent or increased production of sea ice, since no relaxation to observed salinities is specified on the Antarctic shelves. The difference pattern of annual mean net ice production (Figure 4) between the two experiments shows that increased ice production occurs only in the Ross Sea, while in the Weddell Sea the net ice production has decreased due to a stronger inflow of warm shelf water from the east (1.6 Sv, not shown). The net annual sea ice production at all coastal cells in the Southern Ocean (meridional extent ca. 308 km) is 56 cm in the bbl experiment and 61 cm in the control experiment. Both values are near the formation rates required by the observed salinity budget (Toggweiler and Samuels 1995).

In the Southern Ocean, the differences in convective activity between the bbl and the control experiment show a decrease of vertical convection in the deep water of the Weddell and the Ross Sea, and increased activity in the shallow regions near the coast (Figure 5a). Similar to the finding southeast of Greenland, this increased coastal convection is a consequence of more efficient downslope transport of dense bottom water when the bbl parameterization is included (Figure 5b). The decrease of the spurious deep-reaching open-ocean convection is most obvious in the Ross Sea. In the real world, open-ocean convection in the Southern Ocean is trapped at the surface since the salinity stratification is restored when the newly formed ice is melted by the heat brought convectively to the surface (Martinson 1990). In coarse ocean models, however, open ocean convection often reaches from the surface to some 1000 m down into the CDW layer. This leads to dilution of the deep water by fresh surface water, and thus to a too fresh deep water mass when open ocean convection is strong in the models.

Figure 6 shows the bottom temperatures in the Weddell Sea. A tongue of very cold water extends from the western slope towards the east. The minimum value of the bbl experiment is near -1.4^{o}C, almost 1^{o}C colder than in the control experiment. Maximum values of -0.2 to -0.4^{o}C are simulated at the continental break of the eastern Weddell Sea. This pattern compares well with synoptic observations (e.g. Foster and Carmack 1975, their Fig. 13), The bottom salinity, on the other hand, is too fresh by about 0.1 psu and did not change significantly with the bbl scheme. It must be kept in mind, however, that a comparison between different data sets crucially depends on the layer thicknesses used. The temperature maximum in the eastern Weddell Sea is caused by the advection of relatively warm water from the east in the Wed-

dell Sea gyre. This gyre is stronger in the bbl experiment (10%) and suppresses formation of bottom water there. This lack of bottom water formation is in agreement with observation (Fahrbach et al. 1994). The Weddell Sea gyre is convergent above and divergent below 2500 m in both experiments. Below 3500 m, the divergence is 5.5 Sv in the bbl experiment, another 6 Sv divergence is simulated between 2500 m and 3500 m. These values are 5 % larger than in the control experiment. The divergence below 3500 m compares well with Weddell Sea Bottom Water formation rates estimated from direct observation (Muench and Gordon 1995). They are smaller than those obtained by Campin and Goose (1999). However, the divergence in HOPE-G referred to here does not contain the effect of the bbl with is parameterized as a diffusive/convective transport. By contrast, the calculation of Campin and Goose (1999) who obtained 8 Sv includes the effect of their bbl, which is advective. Again, there are only small changes induced in the circulation by the bbl parameterization

Figure 7 shows the temperature distribution of both simulations on a meridional transect through the Ross Sea at 175 E. The isotherms of the bbl experiment are sloping with the continental shelf break, while in the control experiment they are more horizontally or vertically oriented, depending on whether the water is reached by vertical convection or not. In the bbl case, the distribution is more similar to that typically obtained from synoptic observations (Muench and Gordon 1995). However, the bottom layer is thicker than in the observations, since the entire bottom cells belong to the boundary layer in HOPE-G.

Figure 8 demonstrates how the water circulates globally. Despite the rather large impact of the slope convection on the water mass characteristics, the vertical streamfunction has not changed much. The reduction of the maximum downward transport near 60 N reflects a weakened overturning in the North Atlantic. However, since the upwelling of NADW between 45 N and 25 N is reduced by about the same amount, the outflow of NADW at 30 S is almost unchanged (10 Sv). With his idealized model of the North Atlantic, Lohmann (1998) also obtained a reduced maximum in the overturning streamfunction with the 'slope convection' included, and no significant reduction of the outflow across the equator. This is in contrast to the result of Campin and Goose (1999), who obtained a weakened outflow at 30 S and an essentially unchanged maximum overturning in the North Atlantic. However, while outflow obtained by Campin and Goose in their control run is larger than indicated by observations, the HOPE-G control simulation underestimates the outflow by about the same amount. The formation rate of NADW inferred from observations is 13 to 15 Sv with an addition of 4 to 5 Sv of upwelled AABW. There seems to be a close correspondence of the formation rate and the outflow into the Southern Ocean (Schmitz and McCartney 1993). The upwelling of NADW in the North Atlantic in numerical models is thought to balance spurious horizontal diffusion near the western boundary current (Böning et al. 1995). The decrease of the ratio of formation and outflow of NADW can be considered as a success of the bbl scheme.
Again, there are differences in the model forcing which complicate a direct comparison with Campin and Goose (1999). They restore the SST north of 65 N to climatological winter values all year long. This strengthens the deep-water production and the overturning in the North Atlantic.

The global Southern Ocean coastal overturning cell is almost unchanged. The seemingly stronger ventilation, if judged from water mass characterics, is rather due to less dilution of the dense water on its way into the deep ocean than to increased ventilation rates.
Finally the global density profile is shown in Figure 9a for both experiments and can directly be compared with that shown by Campin and Goose (1999). The density in the deep ocean has increased in both models by about the same amount. However, in contrast to the results of Campin and Goose (1999) it has become slightly larger than the climatological values in HOPE-G. Campin and Goose (1999) show almost no changes caused by their bbl parameterisation above 1800 m. In HOPE-G, however, the global density profile has increased at all depths below 700 m which can explain the small changes found in the large scale circulation. More details are seen when differences between the simulated profiles and the climatology are displayed. In the Pacific Ocean (Figure 9b), the density error has increased below 2000 m, in the influence domain of the AABW. This increase is due to a drop of temperature, while the salinity profile is unchanged (not shown). An improvement is obtained below 1500 m in the Indian Ocean (Figure 9c). These layers are strongly influenced by deep water of Atlantic origin entering the Indian Ocean from the west and profit from the cooler and denser characteristics of the latter.

4 Summary and conclusions

A bottom boundary layer parameterization scheme has been implemented in a global ocean general circulation depth-coordinate model. It is known that this type of models is not able to appropriately capture certain aspects of the formation of deep water masses, which are, however, important for an accurate simulation of the world ocean climate. In particular, depth-coordinate models, having their grid aligned with geopotential surfaces involve too much dilution of dense bottom water with lighter ambient water when the water descends topographic slopes on its way from the formation region into the deep ocean.

The bbl parameterization describes the downslope flow as a directional turbulent mixing process, similar to the parameterization of convective overturning of hydrostatically unstable water columns. Horizontally neighboring bottom cells are mixed when they belong to different layers and when the dense water lies above the lighter water mass, i.e. dense water is mixed downslope. With regard to the many numerical and observational studies, which state the numerous processes involved in downslope flow and their potentially large (and partially counteracting) impact on transport rates, which are not and will not be resolved in the near future in global ocean models, no dependence of the strength of the mixing on the state of the ocean is included. The attraction of the formulation adopted here is by its conceptional simplicity. It does not involve new tunable parameters, it is computationally efficient and easy to implement into existing OGCMs.

Two model versions, with and without the new scheme included, are integrated and their results compared against each other, against observations, and against the results of Campin and Goose (1999)

obtained with a similar study. The scheme is implemented into an ocean model which has a high resolution regionally in the tropics since it is used as a component model in coupled ocean-atmosphere climate simulations. It is thus expensive to integrate. Therefore, experiments have been run for 709 years only. Other, longer integrations of the model have shown, however, that this period is sufficiently long to arrive at near-equilibrium.

The locations where downslope transport is simulated by the scheme correspond remarkably well with those where downslope flow is observed directly or indirectly. These are the Weddell and Ross Seas as well as some smaller sites near the Antarctic coast, the Greenland-Scotland ridge system, and in the Strait of Gibraltar. In the Arctic Ocean, downslope transport is simulated only in the Kara Sea, where the sea ice growth rates are large.Wherever such slope flow is simulated it improves the local water mass characteristics. Some downslope flow is also simulated in the eastern Mediterranean and in the Bering Strait, though without significant impact on the model results.

The new scheme improves several large-scale features of the model climatology. The NADW, which is too salty without the scheme, becomes fresher through a larger admixture of fresh water south of the Denmark Strait and near Iceland on the Iceland-Faeroer Ridge. Also, the Mediterranean outflow is slightly reduced and finds its level of neutral density at a deeper level in accord with observations. Another feature which is improved by the bbl parameterization is the ventilation of the abyssal Atlantic Ocean by AABW from the south. This ventilation is too weak without the scheme and thus the bottom water in the Atlantic Ocean is too warm. However, the dense bottom water formed in the Southern Ocean is too fresh and too cold, so that the strengthened ventilation causes a cold and fresh bias in the water that fills the deepest layers of the Atlantic Ocean.

The water formed on the southern high latitude shelves can be made more saline by a number of processes. The most important is perhaps the net production of sea ice. The simulated growth rates cannot be compared with direct observations since the latter do not exist. However, if compared with growth rates derived indirectly from salinity budgets on the shelves, they do not appear to be unrealistic, at least near the coast. The atmosphere model data, on the other hand, which drive the ocean, are known to give an underestimated heat loss in the Southern Ocean, so the ice growth rates could be underestimated due to the forcing.

With the coarse resolution of the model grid, details of the shelf topography which are considered important for deep water formation, cannot be resolved. Examples are submarine ridges on the shelf which form pools where the brine rejected during freezing of sea ice can accumulate. In such pools, water can gain a higher salinity before it spills over the sills near the shelf break. This feature cannot be simulated in coarse resolution OGCMs where the bathymetry is not resolved in such details. If this process were included, and if the downslope transport rates could thereby be reduced, giving a more saline overflow at the same temperature, AABW would become warmer and saltier.

Coarse resolution ocean models often simulate too strong open ocean convection, reaching from the surface deep to the warm CDW layer. Under the conditions in the Southern Ocean, this process serves as an

upward pump of heat and salt, and renders the deep water that flows onto the shelves too cold and too fresh. Consequently, the dense water that is a mixing product of dense shelf and slope water and CDW also becomes too fresh and too cold. The open ocean convection is reduced with the bbl scheme, in particular in the Ross Sea. The slope water formed there is more saline and the water that settles in the deep Pacific has about the same salinity despite the additional ventilation which makes the water colder.
The bbl scheme does not have a strong impact on the general circulation. It does not strengthen the overturning of NADW. In the contrary, in the North Atlantic, the exchange through straits where downslope flow is simulated is weaker since the pressure gradient is reduced by the downslope transport. Transport values elsewhere are changed by a few per cent only. An exception is the ventilation associated with the Southern Ocean, which is increased from 3 Sv to 4 Sv in the Atlantic and by 0.8 Sv from 9 Sv in the Pacific.
Most of the results are in agreement with other model studies as far as a comparison is possible. The results of these sensitivity studies are confirmed despite a number of differences in the model formulations and the parameterizations of the downslope transport. The impact on the model climatology is similar to that described by Campin and Goose (1999), the only other study we know of, which uses a global model with realistic topography.

Acknowledgement

The experiments have been integrated on a NEC SX-4 in a joint project of MPI and NEC European Supercomputer Systems, NEC Deutschland GmbH. We thank the staff of NEC for their support for keeping the model running. Special thanks are due to Achim Stössel for useful comments on the manuscript

5 References

Aagaard, K., J. H. Swift, and E. C. Carmack, 1985: Thermohaline circulation in the Arctic Mediterranean Sea. J. Geophys. Res., 90, 4833-4846.

Adcroft, A., C. Hill, and J. Marshall, 1997: Representation of Topography by Shaved Cells in a Height Coordinate Ocean Model. Mon. Weath. Rev., 125, 2293-2315.

Baines, P. G. and S. Condie, 1998: Observations and modeling of Antarctic downslope flow: a review. In: Ocean, ice, and atmosphere: interactions at the Antarctic continental margin. Eds. S. S. Jacobs and R. F. Weiss, Amer. Geophys. Union, Washington DC, 29-49.

Beckmann, A. and R. Döscher, 1997: A method for improved representation of dense water spreading over topography in geopotential-coordinate models. J. Phys. Oceanogr., 27, 581-591.

Böning C. W., W. R. Holland, F. O. Bryan, G. Danabasoglu, and J. C. McWilliams, 1995: An overlooked problem in model simulations of the thermohaline circulation and heat transport in the Atlantic Ocean. J. Climate, 8, 515-523.

Bryden, H. and T. H. Kinder, 1991: Steady two-layer exchange through the Strait of Gibraltar. Deep-Sea Res., Vol. 38, 5445-5463.

Dickson, R. R. and J. Brown, 1994: The Production of North Atlantic Deep Water: Sources, rates, and pathways. J. Geophys. Res., 99 (C6), 12,319-12,341.

Drijfhout S. S., C. Heinze, M. Latif, and E. Maier-Reimer, 1996: Mean Circulation and Internal Variability in an Ocean Primitive Equation Model. J. Phys. Oceanogr., 26(4), 559-580.

England, M. H., 1993: Representing the global-scale water masses in ocean general circulation models. J. Phys. Oceanogr., 23, 1523-1552.

Fahrbach, E., R. G. Peterson, G. Rohardt, P. Schlosser, and R. Bayer, 1994: Suppression of bottom water formation in the southeastern Weddell Sea. Deep-Sea Res., 41(2), 389-411.

Fohrmann, H., J. O. Backhaus, F. Blaume, and J. Rumohr, 1998: Sediments in bottom arrested gravity plumes : Numerical case studies. J. Phys. Oceanogr., 28, 2250-2274.

Foster, T. D. and E. Carmack, 1976: Frontal zone mixing and Antarctic Bottom Water formation in the southern Weddell Sea. Deep-Sea Res., 23, 301-317.

Frey, H., M. Latif, and T. Stockdale, 1997: The Coupled GCM ECHO-2. Part I: The Tropical Pacific. Mon. Wea. Rev., 125, No. 5, 703-720.

Hibler III, W.D., 1979: A dynamic thermodynamic sea ice model. J. Phys. Oceanogr., 9, 815-846.

Jungclaus, J. H., J. O. Backhaus, and H. Fohrmann, 1995: Outflow of dense water from the Storfjord in Svalbard: A numerical model study. J. Geophys. Res., 100(C12), 24,719-24,728.

Jungclaus, J. H. and G. L. Mellor, 1999: A three-dimensional model study of the Mediterranan outflow. J. Mar. Sys., Vol. 651.

Killworth, P. D., 1977: Mixing on the Weddell Sea continental slope. Deep-Sea Res., 24, 427-448.

Killworth, P. D., 1983: Deep convection in the world ocean. Rev. Geophys. 21, 1-26.

Killworth, P. D. and N. R. Edwards, 1999: A turbulent bottom boundary layer code for use in numerical models. J. Phys. Oceanogr., 29, 1221-1238.

Legutke, S., 1991: Numerical experiments relating to the “Great Salinity Anomaly” of the seventies in the Greenland and Norwegians seas. Progr. Oceanogr. Vol. 17, 341-363.

Legutke, S., E. Maier-Reimer, A. Stössel, and A. Hellbach, 1997: Ocean - sea-ice coupling in a global general circulation model. Annals of Glaciology, 25, 116-120.

Legutke, S. and E. Maier-Reimer, 1999: Climatology of the HOPE-G Global Ocean General Circulation Model. Technical report, No. 21, German Climate Computer Centre (DKRZ), Hamburg, 90 pp (www.dkrz.de/dkrz/dkrz99.html#PUB).

Levitus, S., R. Burgett, and T. P. Boyer, 1994: World Ocean Atlas. Vol. 3, Salinity and Vol. 4, Temperture. NOAA Atlas NESDIS 3/4, U. S. Government Printing Office, Washington, DC.

Lohmann, G., 1998: The Influence of a Near-Bottom Transport Parameterization on the Sensitivity of the Thermohaline Circulation. J. Phys. Oceanogr,, Vol. 28, p. 2095-2103.

Luyten, J., M. McCartney, and H. Stommel, 1993: On the Sources of North Atlantic Deep Water. J. Phys. Oceanogr., 23, 1885-1892.

Lynn, R. J. and J. L.Reid, 1968: Characteristics and circulation of deep and abyssal waters. Deep-Sea Res., 15, 577-598.

Marsland, S. J. and J.-O. Wolff, 2000: On the sensitivity of Southern Ocean sea ice to the surface freshwater flux: A model study. J. Geophys. Res., accepted 27 pp + 15 figs..

Martinson, D.G., 1990: Evolution of the Southern Ocean winter mixed layer and sea ice: Open ocean deepwater formation and ventilation. J. Geophys. Res., 95(C7), 11641-11654.

Muench, R.D. and A. L. Gordon, 1995: Circulation and transport of water along the western Weddell Sea margin, J. Geophys. Res., 100, 18,503-18,515.

Parkinson, C. L. and W. M. Washington, 1979: A large-scale numerical model of sea ice. J. Geophys. Res., 84(C1), 311-337.

Price, J F. and M. O'Neil Baringer, 1994: Outflows and deep water productions by marginal seas. Progs. Oceanogr., 33, 161-200.

Price, J F., M. O'Neil Baringer, R. G. Lueck, G. C. Johnson, I. Ambar, G. Parilla, A. Cantos, M. A. Kennelley, and T. B. Sanford, 1993: Mediterranean mixing and dynamics. Science, 159, 1277-1282.

Reid, J. L., 1979: On the contribution of the Mediterranean outflow to the Norwegian-Greenland Sea. Deep-Sea Res., 26, 1199-1223.

Rhein, M. and H. H. Hinrichsen, 1993: Modification of Mediterranean water in the Gulf of Cadiz, studied with hydrographic, nutrient, and clorofluoromethane data. Deep-Sea Res., 40, 267-291.

Rintoul S. R., 1998: On the Origin and Influence of Adelie Land Bottom Water. In: Ocean, Ice, and Atmosphere: Interactions at the Antarctic Continental Margin, Ed.: S. S. Jacobs and R. F. Weiss, Antarctic Research Series, Washington D. C., 151-171.

Roeckner, E., K. Arpe, L. Bengtsson, M. Christoph, M. Claussen, L. Dümenil, M. Esch, M. Giorgetta, U. Schlese, and U. Schulzweida, 1996: The atmospheric general circulation model ECHAM-4: Model description and simulation of present-day climate. Reports of the Max-Planck-Institute, Hamburg, No. 218, 90 pp (www.mpimet.mpg.de/deutsch/Sonst/Reports/index.html).

Rudels, B., E. P. Jones, L. G. Anderson, and G. Kattner, 1994: On the intermediate depth water in the Arctic Ocean., in The Polar Oceans and their Role in Shaping the Global Environment, ed. by O. M. Johannessen, R. D. Muench, and J. E. Overland, Washington D. C., 33-46.

Schauer, U., R. D. Muench, B. Rudels, and L. Timokhov, 1997: Impact of eastern Arctic shelf waters on the Nansen Basin intermediate layers. J. Geophys. Res., 102, 3371-3382.

Schmitz, W. J. and M. S. McCartney, 1993: On the North Atlantic circulation. Rev. Geophys., 31(1), 29-49.

Stössel, A. and S. J. Kim 1998: An interannual Antarctic sea-ice - ocean mode. Geophys. Res. Lett., 25(7), 1007-1010.

Toggweiler, J. R. and B. Samuels, 1995: Effect of Sea Ice on the Salinity of Antarctic Bottom Waters. J. Phys. Oceanogr., Vol. 25, 1980-1997.

UNESCO, 1983: Algorithms for computation of fundamental properties of sea water. UNESCO Techn-cal Papers in Marine Science, No. 44.

Hibler III, W.D., 1979: A dynamic thermodynamic sea ice model. J. Phys. Oceanogr., 9, 815-846.

Wolff, J.-O., E. Maier-Reimer, and S. Legutke, 1997: The Hamburg Ocean Primitive Equation Model. Technical report, No. 13, German Climate Computer Center (DKRZ), Hamburg, 98 pp (www.dkrz.de/dkrz/dkrz99.html#PUB).

6 Figure Captions

Figure 1 (a) Difference (bbl minus control) of potential energy released by vertical convective adjustment in the North Atlantic.
(b) Change of potential energy caused by the bbl parameterization in the North Atlantic.
(c) Difference (bbl minus control) of potential energy changes caused by total (vertical and downslope) convective adjustment in the Barents and Kara Seas.
Contour interval is 2.5 10^{-3} W/m^2, in (a) and (b) and 0.2 10^{-3} W/m^2 in (c). Negative contours are dashed.

Figure 2 Simulated vertical profiles of (a) potential temperature, (b) salinity, and (c) in-situ density error (relative to the Levitus et al. (1994) climatology) in the North Atlantic (areal mean between 46 W and 36 W, and 24 N and 36 N). The full lines are for the run with the bbl parameterization included and the dashed lines for the control run without bbl parameterization. Units are ^{o}C, psu, and kg/m^3 respectively.

Figure 3 Difference (bbl minus control) of zonal-mean salinity in the Atlantic Ocean.

Figure 4 Difference (bbl minus control) of net sea ice growth in the Southern Ocean. Contour interval is 20 cm.

Figure 5 (a) Difference (bbl minus control) of potential energy released by vertical convective adjustment in the Southern Ocean.
(b) Change of potential energy caused by the bbl parameterization in the Southern Ocean.
Contour interval is 2.5 10^{-3} W/m^2, negative contours are dashed.

Figure 6 Simulated bottom potential temperature (values in lowest grid cell) in the Weddell Sea for depths greater than 2000 m : (a) control rexperiment and (b) bbl experiment. Contour interval is 0.2 ^{o}C, negative contours are dashed. The dash-dot contours are bathymetric isolines (C.I.=1000 m). Shaded areas have water depth skallower than 2000 m.

Figure 7 Potential temperature on a meridional vertical section at 175 E in the Ross Sea simulated in (a) the bbl experiment and (b) the control experiment. Contour interval is 0.2 ^{o}C, negative contours are dashed.

Figure 8 Global vertical overturning streamfunction simulated in the (a) bbl experiment and (b) the control experiment. Contour interval is 2 Sv, negative contours are dashed.

Figure 9 (a) Global mean vertical profiles of density minus a reference profile calculated with 4^{o}C and 34 psu. (bbl experiment : full line; control experiment: dashed line; Levitus et al. (1994) atlas: dot-dashed line)
(b) Density error (relative to the Levitus et al. (1994) climatology) in the (b) Pacific and (c) Indian Ocean. The full lines are for the run with the bbl parameterization included and the dashed lines for the control run without bbl parameterization. Units are ^{o}C, psu, and kg/m^3 respectively.

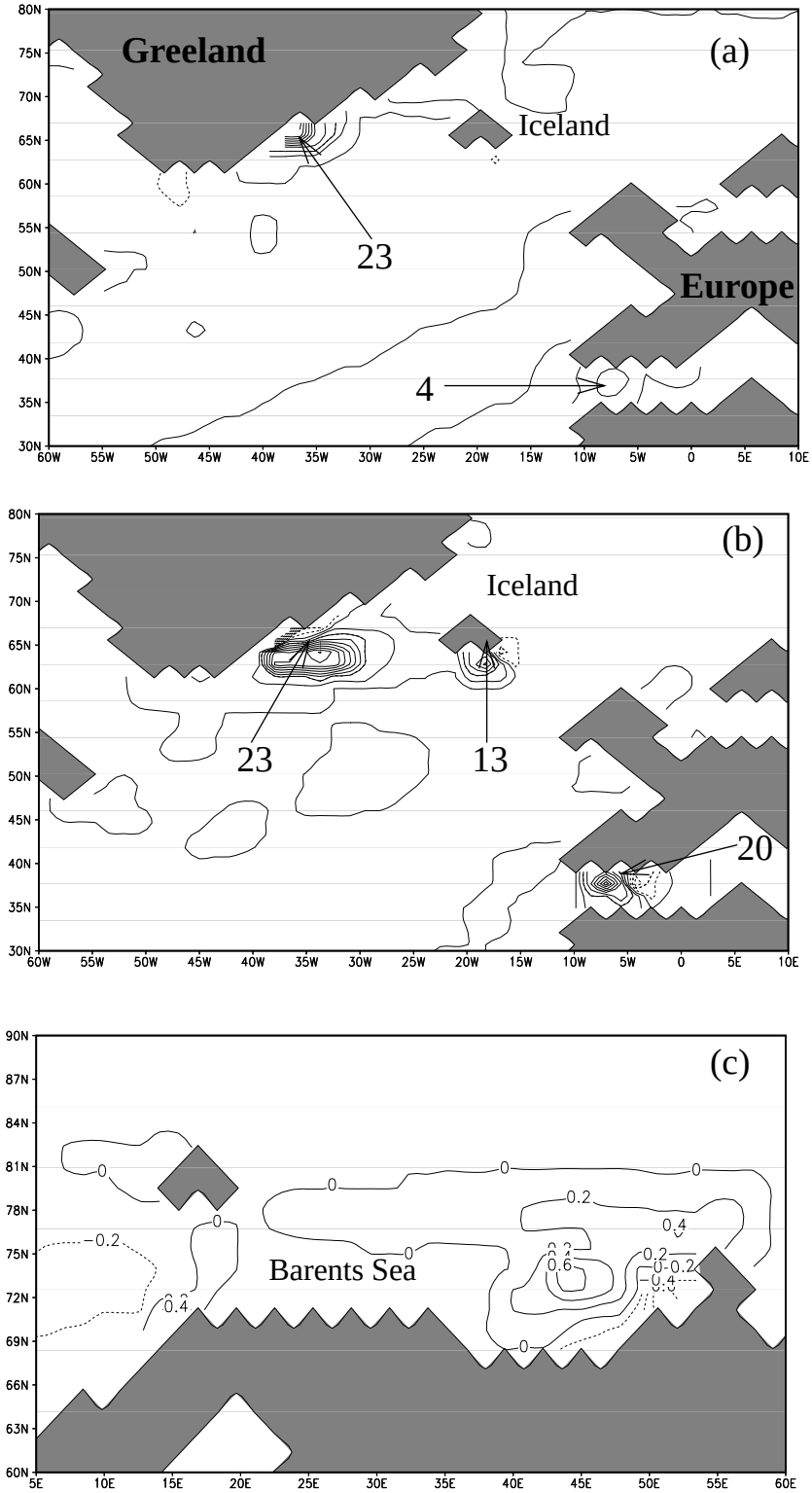

Figure 1
(a) Difference (bbl minus control) of potential energy released by vertical convective adjustment in the North Atlantic.
(b) Change of potential energy caused by the bbl parameterization in the North Atlantic.
(c) Difference (bbl minus control) of potential energy changes caused by total (vertical and downslope) convective adjustment in the Barents and Kara Seas.
Contour interval is 2.5 10^{-3} W/m^2, in (a) and (b) and 0.2 10^{-3} W/m^2 in (c).
Negative contours are dashed.

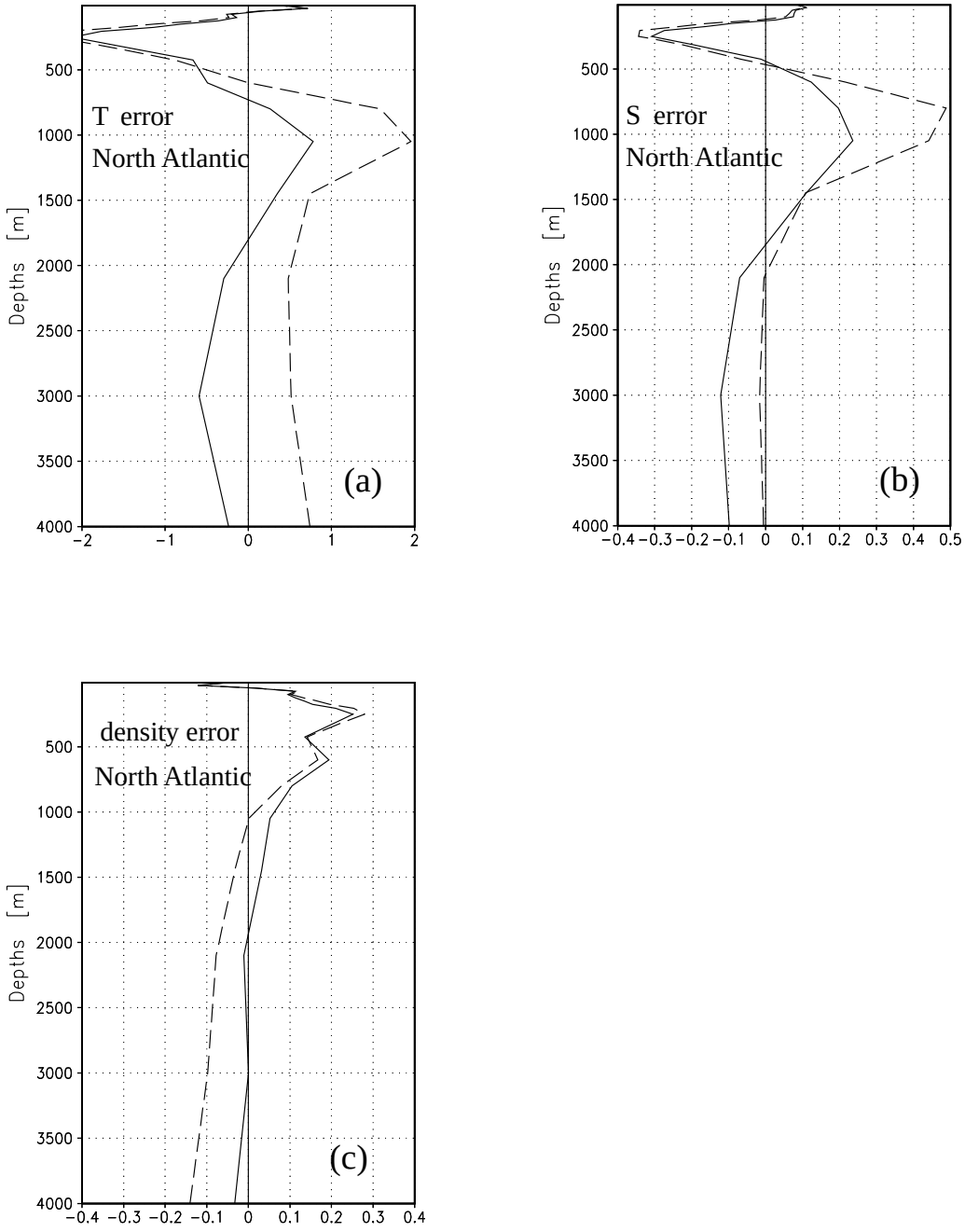

Figure 2
Simulated vertical profiles of (a) potential temperature, (b) salinity, and (c) in-situ density error (relative to the Levitus et al. (1994) climatology) in the North Atlantic (areal mean between 46^{o}W and 36^{o}W, and 24^{o}N and 36^{o}N). The full lines are for the run with the bbl parameterization included and the dashed lines for the control run without bbl parameterization. Units are ^{o}C, psu, and kg/m^{3}, respectively.

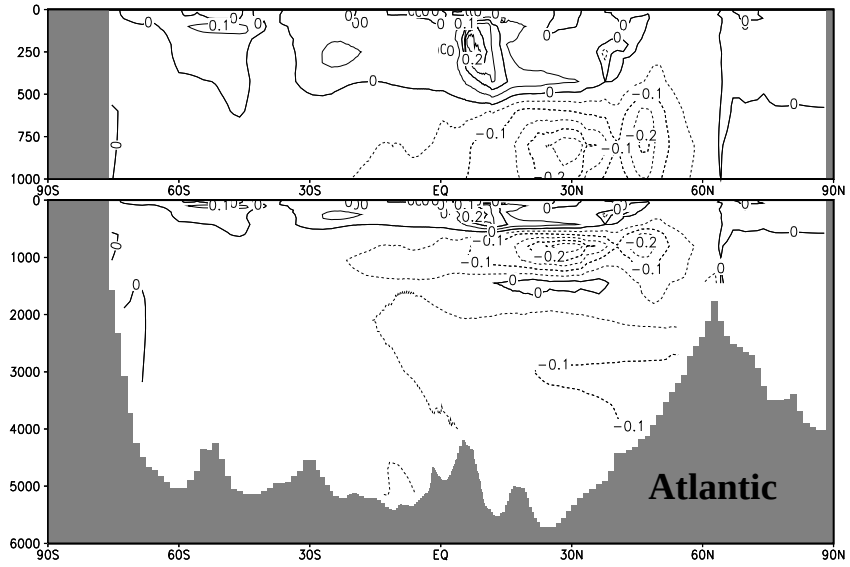

Figure 3
Difference (bbl minus control) of zonal-mean salinity in the Atlantic Ocean.

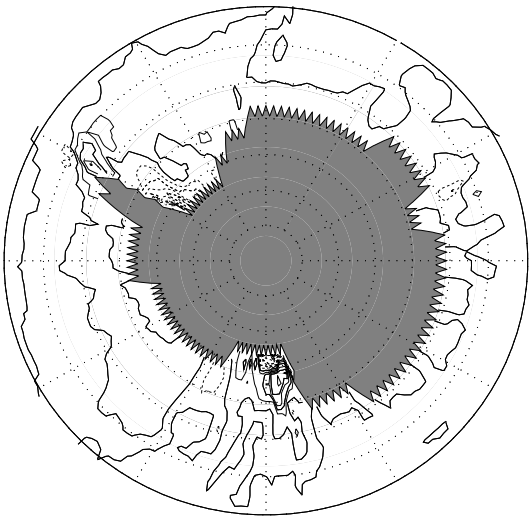

Figure 4
Difference (bbl minus control) of net sea ice growth in the Southern Ocean. Contour interval is 20 cm.

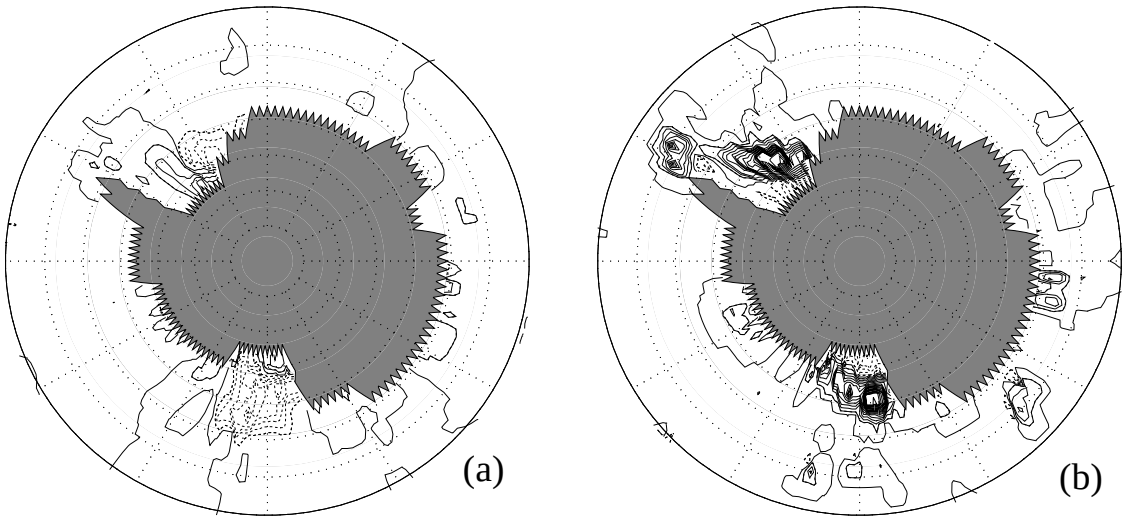

Figure 5
(a) Difference (bbl minus control) of potential energy released by vertical convective adjustment in the Southern Ocean.
(b) Change of potential energy caused by the bbl parameterization in the Southern Ocean.
Contour interval is 2.5 10^{-3} W/m^2, negative contours are dashed.

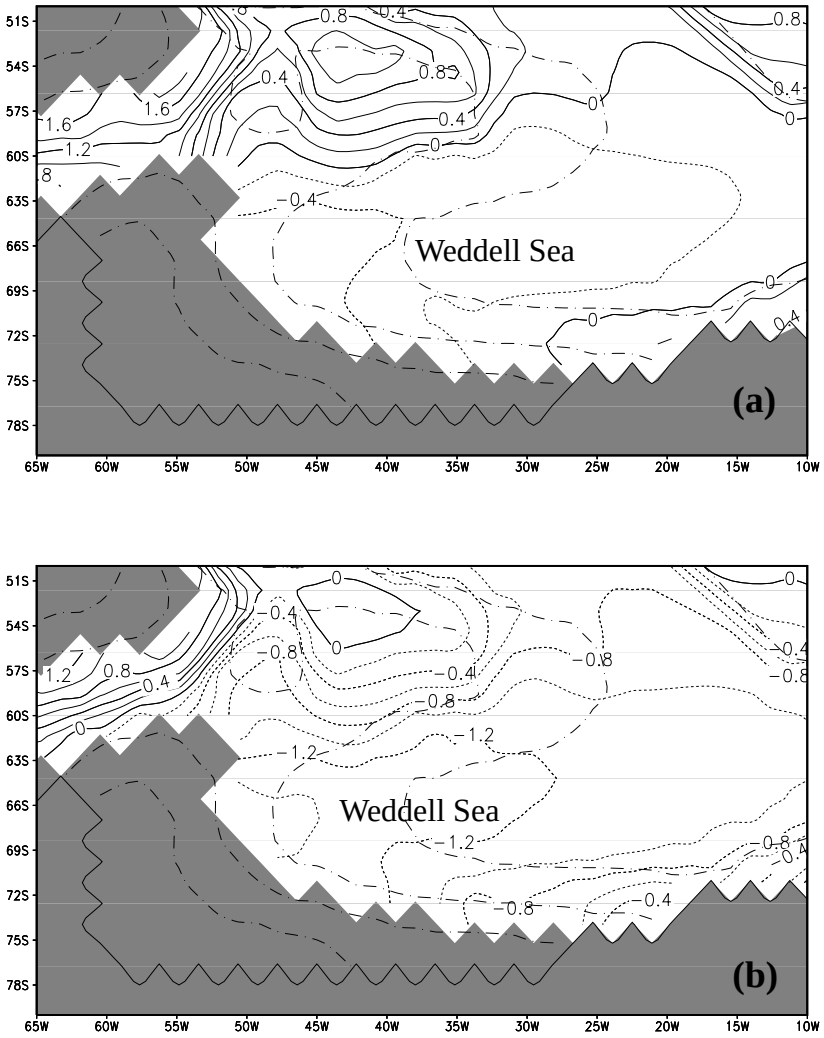

Figure 6
Simulated bottom potential temperature (values in lowest grid cell) in the Weddell Sea for depths greater than 2000 m : (a) control experiment and (b) bbl experiment. Contour interval is 0.2^{o}C, negative contours are dashed. The dash-dot contours are bathymetric isolines (contour interval 1000 m). Shaded areas have water depth shallower than 2000 m.

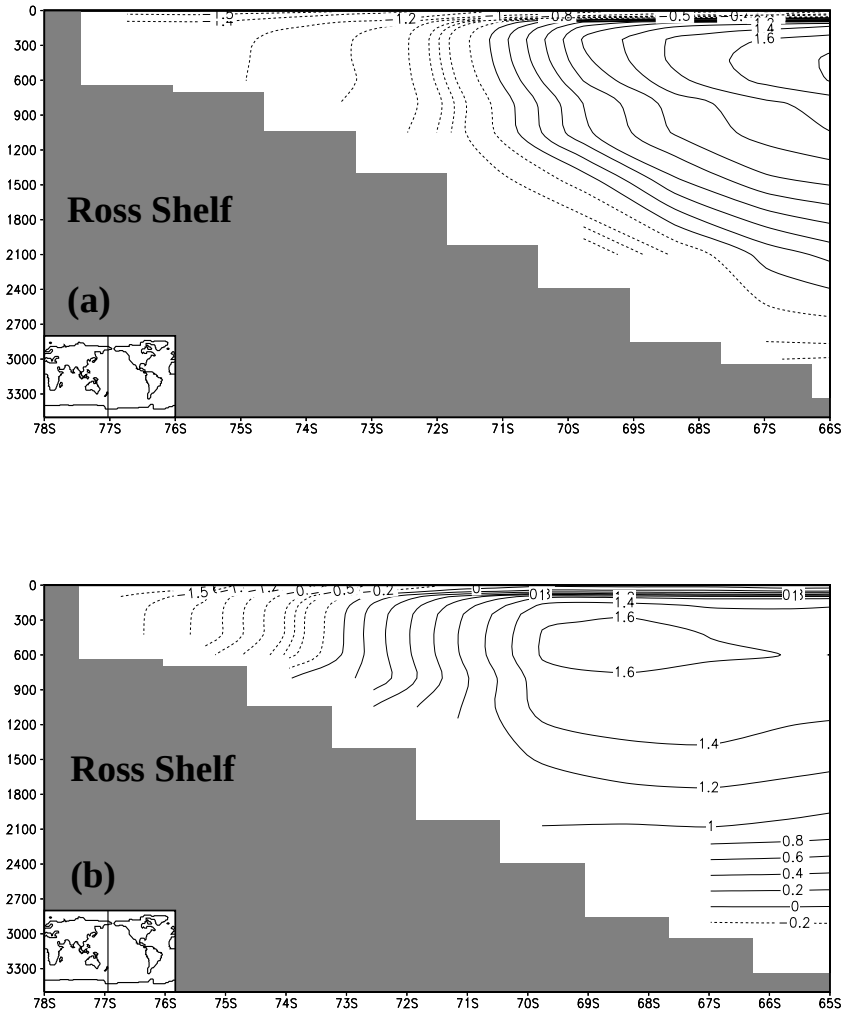

Figure 7
Potential temperature on a meridional vertical section at 175^{o}E in the Ross Sea simulated in (a) the bbl experiment and (b) the control experiment. Contour interval is 0.2^{o}C, negative contours are dashed.

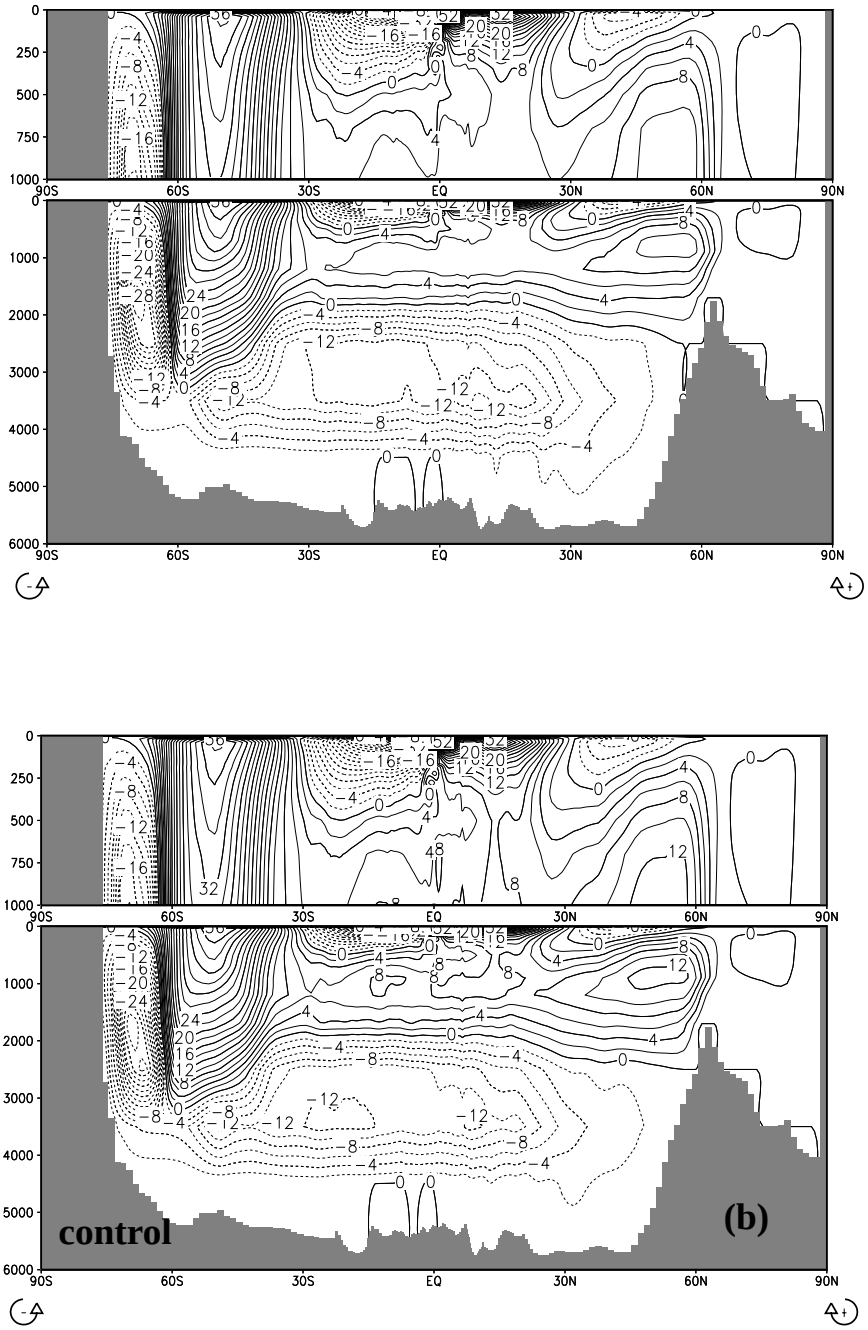

Figure 8
Global vertical overturning streamfunction simulated in the (a) bbl experiment and (b) the control experiment. Contour interval is 2 Sv, negative contours are dashed.

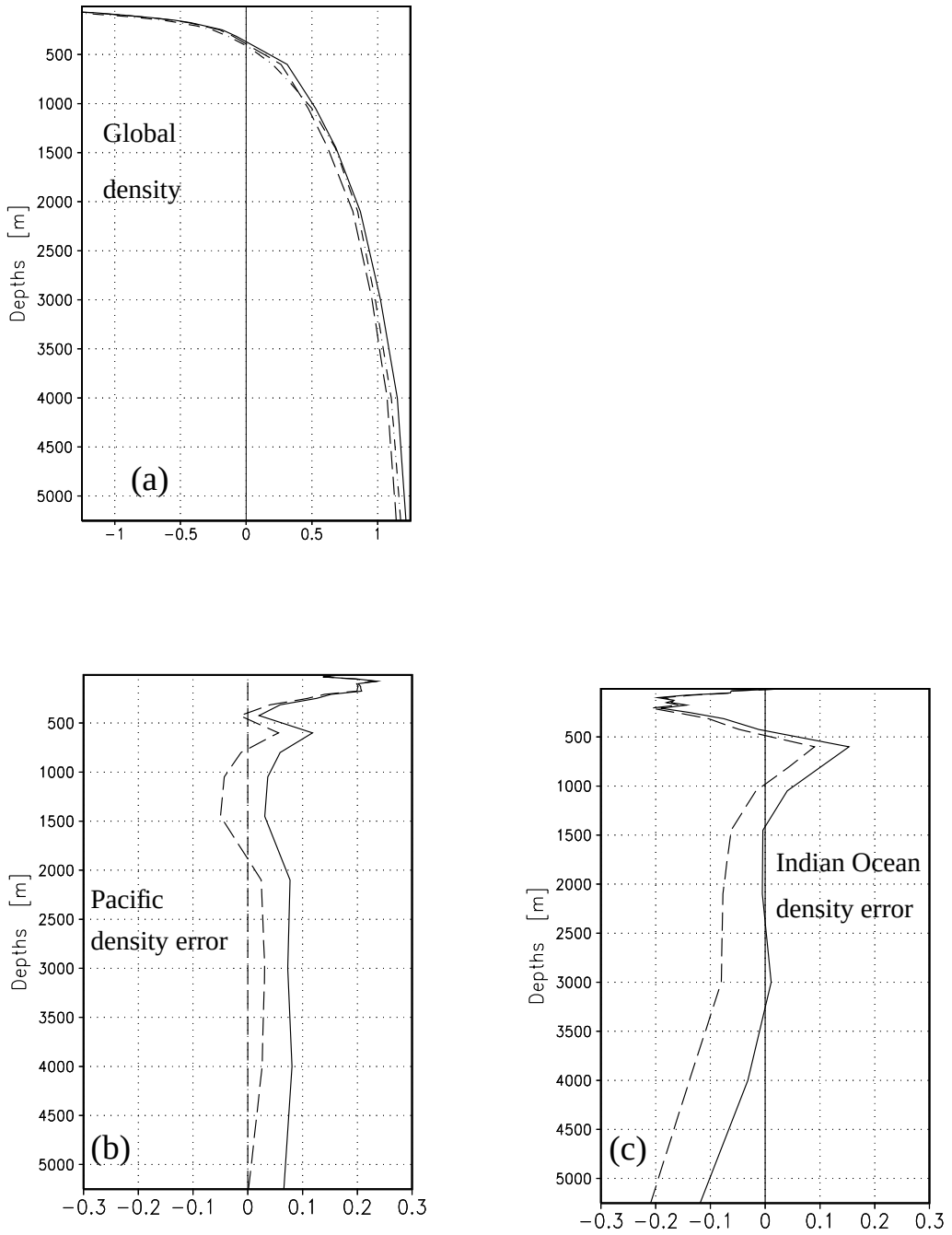

Figure 9
(a) Global mean vertical profiles of density minus a reference profile calculated with 4^{o}C and 34psu (bbl experiment: full line; control experiment: dashed line; Levitus et al. (1994) climatology: dot-dashed line).
(b)-(c) Density error (relative to the Levitus et al. (1994) climatology) in the (b) Pacific and (c) Indian Ocean. The full lines are for the run with the bbl parameterization included and the dashed lines for the control run without bbl parameterization. Units are kg/m^3